

SP1 Promotes HDAC4 Expression and Inhibits HMGB1 Expression to Reduce Intestinal Barrier Dysfunction, Oxidative Stress, and Inflammatory Response after Sepsis

Zhen-Mi Liu^a Xi Wang^a Chen-Xi Li^a Xue-Yan Liu^a Xiao-Jing Guo^b Yang Li^c
You-Lian Chen^a Hong-Xing Ye^a Huai-Sheng Chen^a

^aDepartment of Critical Care Medicine, Shenzhen People's Hospital, The Second Clinical Medical College of Jinan University, The First Affiliated Hospital of South University of Science and Technology, Shenzhen, PR China;

^bDepartment of Pathology, Shenzhen People's Hospital, The Second Clinical Medical College of Jinan University, The First Affiliated Hospital of South University of Science and Technology, Shenzhen, PR China; ^cDepartment of Gastrointestinal Surgery, Shenzhen People's Hospital, The Second Clinical Medical College of Jinan University, The First Affiliated Hospital of South University of Science and Technology, Shenzhen, PR China

Keywords

Specificity protein-1 · Histone deacetylase 4 · High mobility group box 1 · Sepsis · Intestinal barrier dysfunction · Oxidative stress · Inflammatory response

Abstract

As a serious and elusive syndrome caused by infection, sepsis causes a high rate of mortality around the world. Our investigation aims at exploring the role and possible mechanism of specificity protein-1 (SP1) in the development of sepsis. A mouse model of sepsis was established by cecal ligation perforation, and a cellular model was stimulated by lipopolysaccharide (LPS), followed by determination of the SP1 expression. It was determined that SP1 was poorly expressed in the intestinal tissues of septic mice and LPS-treated cells. Next, we examined the interactions among SP1, histone deacetylase 4 (HDAC4), and high mobility group box 1 (HMGB1) and found that SP1 bound to the HDAC4 promoter to upregulate its expression, thereby pro-

moting the deacetylation of HMGB1. Meanwhile, gain- or loss-of-function approaches were applied to evaluate the intestinal barrier dysfunction, oxidative stress, and inflammatory response. Overexpression of SP1 or underexpression of HMGB1 was observed to reduce intestinal barrier dysfunction, oxidative stress, and inflammatory injury. Collectively, these experimental data provide evidence reporting that SP1 could promote the HDAC4-mediated HMGB1 deacetylation to reduce intestinal barrier dysfunction, oxidative stress, and inflammatory response induced by sepsis, providing a novel therapeutic target for sepsis prevention and treatment.

© 2022 The Author(s).
Published by S. Karger AG, Basel

Introduction

Sepsis is a clinical syndrome manifested by a multi-organ dysfunction caused by dysregulated inflammatory response to infection and remains a major cause of

morbidity and mortality worldwide [1]. Intestinal barrier dysfunction is a vital driver of the development of multiple organ dysfunction syndromes during sepsis [2]. Of note, intestinal barrier dysfunction is the cause of sepsis, it can also be the result of sepsis-induced intestinal barrier dysfunction, and the intestinal barrier dysfunction induced by sepsis increases the fatality rate of sepsis [2, 3]. Additionally, the patients with sepsis present greater oxidative stress which can trigger cell, tissue, and organ damage, causing significant morbidity and mortality [4]. The early diagnosis and stratification of the severity of sepsis are very important, which contribute to timely and specific treatment and thus improve the clinical outcome [5]. However, the diagnosis and severity evaluation of sepsis is complicated due to the highly variable and nonspecific nature of its signs and symptoms [6].

Specificity protein-1 (SP1) belongs to the member of the SP family of transcription factors [7] and is implicated in inflammation and genomic instability as well as epigenetic silencing [8]. In lipopolysaccharide (LPS)-activated macrophages, SP1 can directly bind to the proximal promoter of TRIM59 gene which may serve as a potential therapeutic target for inflammatory diseases [9]. A recent work revealed that SP1 binds to the histone deacetylase 4 (HDAC4) gene promoter sequence and induces the consequent upregulation of HDAC4 mRNA and protein expressions in SH-SY5Y neuroblastoma cells [10]. HDAC4, a class IIa histone deacetylase, is implicated in the regulation of gene expression essential for diverse cellular functions, such as cell growth, survival, and proliferation, and its aberrant expression or activity initiates human diseases [11]. For instance, it has been suggested that HDAC4 and HDAC5 collectively participated in the pathogenesis of stroke and reduced stroke-induced neuronal damage [12]. Intriguingly, HDAC4 has been confirmed to be a potential target for the treatment of sepsis since its overexpression can impair the acetylation and secretion of high mobility group box 1 (HMGB1) in LPS-activated macrophages [13]. Meanwhile, inhibition of HMGB1 has been shown to suppress the early proinflammatory responses in murine sepsis models [14]. Therefore, we hypothesized that SP1 might play a crucial role in inhibiting the sepsis progression via HDAC4-dependent deacetylation of HMGB1. The present study aimed to investigate the association between SP1 and the HDAC4/HMGB1 signaling along with their interactions in intestinal barrier dysfunction, oxidative stress, and inflammatory response following sepsis.

Methods

Establishment of a Sepsis Model through Cecal Ligation Perforation

A total of 48 C57BL/6J male mice (aged 8–12 weeks, Animal Research Center of Shenzhen People's Hospital, The Second Clinical Medical College of Jinan University, The First Affiliated Hospital of South University of Science and Technology) were used for this experiment. The mice were housed individually in specific pathogen-free animal laboratory with humidity of 60–65% and temperature of 22–25°C under a 12-h light/dark cycle. The mice had free access to food and water. The experiment was conducted after 1 week of adaptive feeding, and the health of mice was observed before the experiment.

The mice were then subjected to cecal ligation perforation (CLP) operation ($n = 8$) for the sepsis model establishment. Briefly, anesthesia was induced and the mice were placed on a board in a supine position, whereupon a midline incision was made in the peritoneum and the cecum was exteriorized. The feces of the upper cecum were squeezed to fill the end, and the blood vessels on the mesenteric surface were separated. Next, 50% of the cecum was ligated with sterile No. 4 suture and punctured twice with a 21-G needle, and a small drop of cecal content was extruded. For the Sham-operated mice ($n = 8$), the cecum was exteriorized after laparotomy and then received no treatment. The cecum was then returned to the peritoneal cavity and the abdominal incision closed with sutures. Moreover, 24 h before CLP operation, the mice were injected with lentivirus carrying overexpression-negative control (oe-NC) (10 μg , $n = 8$) and oe-SP1 (10 μg , $n = 8$), as well as CRISPR/Cas9 control and HMGB1^{-/-} plasmids (HMGB1 knockdown plasmids) [15, 16], and 3 days later, the survival of mice was monitored.

Colony-Forming Unit of Peritoneal Lavage

The mice were anesthetized 24 h after CLP operation, and the skin on the abdomen surface was gently cut to fully expose the peritoneum. Then, 3 mL of phosphate-buffered saline (PBS) was absorbed with a syringe and slowly injected into the abdominal cavity through the peritoneum. The peritoneum was gently wiped with sterile cotton swabs, and the peritoneal lavage fluid (PLF) was extracted for bacterial culture. The same procedure was repeated 3 times. Additionally, the mouse heart was fully exposed, and approximately, 200 μL of blood was extracted and stored in a sterile Eppendorf tube for bacterial culture. The PLF and blood were then separately pipetted 50 μL and diluted 6 times with PBS, after which 50 μL of the diluted PLF and blood was uniformly coated on the tryptic soy blood agar plate. Subsequently, the plate was incubated at 37°C for 24 h under aerobic conditions and colony-forming unit was counted.

Enzyme-Linked Immunosorbent Assay

The expression of TNF- α , IL-1 β , and IL-6 in mouse serum and cell supernatant was detected using the enzyme-linked immunosorbent assay (ELISA) kit (Abcam Inc., Cambridge, UK) according to the provided instructions. In short, 0.1 mL of cell supernatant was put into 96-well plates and incubated at 37°C for 1 h. After washing, each well was added with 0.1 mL of freshly diluted enzyme-labeled antibody (titrated dilution) and incubated at 37°C for 0.5–1 h. Next, 0.1 mL of TMB substrate solution was supplemented into each well and incubated at 37°C for 10–30 min, which

was halted by addition of 0.05 mL sulfuric acid (2 M). The optical density value of each well was measured using a microplate reader at 450 nm, and the concentration of TNF- α , IL-1 β , and IL-6 was calculated.

Malondialdehyde and Superoxide Dismutase Measurements

The malondialdehyde (MDA) level and superoxide dismutase (SOD) activity were measured using commercial kits (Nanjing Jiancheng Bioengineering Institute). Briefly, mouse intestinal tissues were prepared into 10% tissue homogenate, which was added with reagents and mixed. The mixture was then subjected to water bath for 40 min at 95°C, and removed and cooled with running water, followed by centrifugation at 2,800–3,200 g for 10 min. The supernatant was collected, whereupon MDA and SOD were assayed. For MDA and SOD measurements in cells, the cells following varied treatments were prepared into 10% homogenate, which was put into a –20°C freezer and repeated freeze-thaw for 3 times. Then, a microscope was used to analyze whether the cells were completely broken. If not, freeze-thaw continued twice and centrifugation was followed at 3,200 g for 15 min. With the supernatant harvested, MDA and SOD were measured.

Hematoxylin-Eosin Staining

Intestinal tissues of mice were extracted and cut into sections, which were dewaxed and rehydrated. Following washing with distilled water, the sections were stained with hematoxylin for 3–8 min, immersed in hydrochloric acid-ethanol, and blued in 0.6% ammonia water. Next, the sections were stained with eosin for 1–3 min after washing with distilled water. Then, the sections were dehydrated, cleared with xylene, air dried, and sealed with neutral balsam. Finally, the sections were observed under a microscope (TE200; Nikon, Tokyo, Japan).

Transmission Electron Microscope

Intestinal tissues were collected 24 h before CLP operation, fixed with 2.5% glutaraldehyde, rinsed with PBS (pH = 7.0), and refixed with 1% osmium tetroxide. Following PBS washing, the tissues were dehydrated with graded ethanol and acetone, paraffin-embedded, and cut into sections. The sections were then stained with 2% saturated uranyl acetate and lead citrate, and observed under a Tecnai G2 TEM (FEI Company, Hillsboro, OR, USA).

Terminal Deoxynucleotidyl Transferase-Mediated dUTP-Biotin Nick End Labeling Assay

Cell apoptosis in the intestinal tissue was measured by the apoptosis detection kit (11684817910; Roche, Basel, Switzerland). Paraffin sections of mouse intestinal tissues were dewaxed with xylene, rehydrated in descending series of alcohol, and treated with proteinase K (20 μ g/mL) at room temperature for 15–30 min. Terminal deoxynucleotidyl transferase-mediated dUTP-biotin nick end labeling (TUNEL) reaction mixture was then prepared, 50 μ L of which was extracted and added to the sections, followed by 1 h of reaction in a wet box under dark conditions. Next, the sections were rinsed 3 times with PBS before observation under a fluorescence microscope (excitation wavelength of 450–500 nm, detection wavelength of 515–565 nm) to determine the apoptotic cells. After the slide was dried, 50 μ L of converter peroxidase was added to the sections, which were covered with slide or sealing film and reacted in a wet box without light expo-

sure for 30 min at room temperature. Thereafter, 50–100 μ L of 3,3'-diaminobenzidine tetrahydrochloride (DAB) substrate was added to the sections for 10 min of reaction, followed by counterstaining with hematoxylin or methyl green. After washing with tap water, the sections were dehydrated, cleared, and mounted. Finally, the sections were observed under a light microscope (DM500; Leica, Wetzlar, Germany) to analyze the apoptosis rate.

Immunohistochemistry

The intestinal tissues of mice were fixed in 4% paraformaldehyde, paraffin-embedded, and cut into 4- μ m-thick sections, which were dewaxed and subjected to microwave antigen retrieval. After PBS washing, the sections were blocked with normal goat serum blocking solution and then immunostained with primary antibodies against SP1 (ab227383, 1:500, Rabbit; Abcam), HDAC4 (ab79521, 1:200, Rabbit; Abcam), and HMGB1 (ab79823, 1:400, Rabbit; Abcam) at 4°C overnight. The following day, secondary antibody donkey anti-rabbit (ab6802, 1:1,000; Abcam) was added to the sections and reacted at room temperature for 30 min, followed by development with 3,3'-diaminobenzidine tetrahydrochloride for 5–10 min. Five representative high-power visual fields were randomly selected and observed under a microscope following hematoxylin counterstaining and balsam blocking. The cells with brown or yellow cytoplasm were considered as positive cells. Image-Pro Plus (version 6; Media Cybernetics, Silver Spring, MD, USA) was used to evaluate the integrated optical density of immunostained samples.

Cell Culture and Transfection

Mouse intestinal epithelial cells MODE-K purchased from Shanghai Huzhen Biotechnology Co., Ltd. were cultured with Roswell Park Memorial Institute 1640 medium (Gibco-BRL, Bethesda, MD, USA) containing 10% fetal bovine serum (Gibco) in a 5% CO₂ incubator (Thermo Fisher Scientific, Waltham, MA, USA) at 37°C. The cells at the logarithmic growth phase were trypsinized and seeded into 6-well plates at a density of 1×10^5 cells/well and culture for 24 h. Upon reaching 75% confluence, the cells were transfected using the Lipofectamine 2000 reagent (Invitrogen, Carlsbad, CA, USA).

Some cells were used as the control, and the remaining were used for cell sepsis model construction by the LPS (1 μ g/mL) method. Before 24 h of LPS treatment, cells were transfected with oe-NC, oe-SP1, oe-HDAC4, oe-SP1 + si-NC, and oe-SP1 + oe-HMGB1. oe-NC, oe-HDAC4, oe-HMGB1, si-NC, and si-HDAC4 were purchased from Shanghai GenePharma Co., Ltd., Shanghai, China. The concentration of transfected siRNA was 50 nm for each group. After transfection, the cells were collected for subsequent experiments.

Reverse Transcription-Quantitative Polymerase Chain Reaction

The total RNA was extracted from cells or tissues with TRIzol reagents (16096020 or AM1561; Thermo Fisher Scientific). A total of 5 μ g RNA was reversely transcribed into cDNA according to the instructions of the reverse transcription-quantitative polymerase chain reaction (RT-qPCR) kit (RR047A; Takara Bio Inc., Otsu, Shiga, Japan). RT-qPCR was then performed using the Fast SYBR Green PCR Kit (Applied Biosystems, Carlsbad, CA, USA) and the ABI PRISM 7300 RT-qPCR system (Applied Biosystems).

All investigations involved at least 3 wells. The primers are shown in online suppl. Table 1 (for all online suppl. material, see www.karger.com/doi/10.1159/000518277). Glyceraldehyde-3-phosphate dehydrogenase (GAPDH) was considered as an internal reference, and the fold changes were calculated by relative quantification ($2^{-\Delta\Delta C_t}$ method).

Western Blot Analysis

Total protein was extracted from cells using enhanced radioimmunoprecipitation assay lysis buffer (Boster Biological Technology Co., Ltd., Wuhan, Hubei, China) containing protease inhibitor, and the concentration was determined using a bicinchoninic acid protein assay (Boster). The protein was then separated by 10% sodium dodecyl sulfate-polyacrylamide gel electrophoresis and electro-transferred onto polyvinylidene fluoride membranes. The membrane was blocked with 5% bovine serum albumin for 1 h at room temperature and probed at 4°C overnight with the following diluted primary antibodies (Abcam): HO-1 (ab68477, 1:10,000, Rabbit), Occludin (ab216327, 1:1,000, Rabbit), SP1 (ab227383, 1:2,000, Rabbit), HDAC4 (ab235583, 1:1,000, Rabbit), HMGB1 (ab18256, 1:500, Rabbit), Acetyl-Lys (ab190479, 1:2,000, Rabbit), GAPDH (ab181603, 1:5,000, Rabbit), and Lamin A (ab133256, 1:10,000, Rabbit). After 3 washes using Tris-buffered saline Tween-20, the membrane was reprobed with the horseradish peroxidase-labeled secondary antibody (goat anti-rabbit, ab205718, 1:1,000; goat anti-mouse, ab205719, 1:1,000; Abcam) for 1 h at room temperature. The bands were visualized using enhanced chemiluminescence (Baoman Biotechnology Co., Ltd., Shanghai, China). With GAPDH and Lamin A as internal references, ImageJ software was used to analyze the gray value.

Flow Cytometry

After 48 h of transfection, the cells were treated with 0.25% trypsin (without EDTA, YB15050057; Shanghai Yubo Biotechnology Co., Ltd., Shanghai, China) and collected in a flow tube, followed by centrifugation and supernatant removal. The cells were washed 3 times with cold PBS, and the supernatant was discarded following centrifugation. According to the instructions of Annexin-V-fluorescein isothiocyanate (FITC) cell apoptosis detection kit (K201-100; BioVision, Milpitas, CA, USA), Annexin-V-FITC, propidium iodide (PI), and 4-(2-hydroxyethyl)-1-piperazineethanesulfonic acid (HEPES) buffer solution were mixed into Annexin-V-FITC/PI staining solution at the ratio of 1:2:50. The cells were then resuspended at a density of 1×10^6 cells per 100 μ L of dye solution and mixed by shaking. After incubation at room temperature for 15 min, 1 mL of 4-(2-hydroxyethyl)-1-piperazineethanesulfonic acid buffer solution (PB180325; Procell Life Science & Technology Co., Ltd., Wuhan, Hubei, China) was added to the cells and mixed. Fluorescence of FITC and PI was initiated by excitation at 488 nm and measured by emission filters at 525 nm (FITC) and 620 nm (PI).

Immunofluorescence Assay

Cells were made crawl on the slide, which was fixed with 4% paraformaldehyde for 15 min, washed 3 times with PBS (3 min per wash), and treated with 0.5% Triton X-100 at room temperature for 20 min. Thereafter, normal goat serum was added on the slide and blocked for 30 min at room temperature. After the blocking solution removal, the slide was probed overnight at 4°C

with primary antibody against HMGB1 (ab18256, 1:500; Abcam). The next day, the slide was reprobed with specific Alexa Fluor 568 or 488 secondary antibody (Invitrogen, Carlsbad, CA, USA) for 2 h and then stained with 3 μ M 4',6-diamidino-2-phenylindole (Sigma-Aldrich Chemical Company, St Louis, MO, USA). Finally, the immunolabeled tissues were observed under a laser scanning confocal fluorescence microscope equipped with Zen software.

Chromatin Immunoprecipitation

Cells were collected and fixed with 1% formaldehyde for 10 min to produce DNA-protein cross-linking. Then, the cells were added with 0.125 M glycine, lysed using radioimmunoprecipitation assay buffer (P0013B; Shanghai Beyotime Biotechnology Co. Ltd., Shanghai, China), and then subjected to ultrasonic treatment to produce 200–700 bp chromatin fragments. Next, a portion of cell lysate was taken out as input and a portion was incubated overnight at 4°C with the antibodies against SP1 (ab231778, 1:200; Abcam) and IgG (ab190475, 1:200; Abcam), both of which had been supplemented with Dynabeads™ Protein G (Thermo Fisher Scientific). After incubation and de-cross-linking, DNA was then eluted, extracted, and stored at –20°C for later use. Subsequently, RT-qPCR was conducted to detect the enrichment in the immune complexes with the primer sequences of 5'CCCAACCTTCT-GACTGACCT' and 5'AGCCCATGAGTCAGAGGTTG-3'. Genome involved in this assay was presented in online suppl. Figure 1.

Dual-Luciferase Reporter Assay

Roche GC-rich PCR kit was utilized to amplify HDAC4 promoter containing multiple Sp1 binding sites from genomic DNA, and the primers used for the construction of HDAC4-PGL3 luciferase reporter were as follows: F: 5'CAT-AGA-TCT-GTG-GGA-GCA-GAC-GGG-CTG-TG-3' and R: 5'CAT-AAG-CTT-CAG-GCT-GGG-CTG-TTC-GG-3'. Then, amplified HDAC4 promoter fragment was cloned into pGL3 vector (Promega, Madison, WI, USA) to produce (–317 to +117) HDAC4-pGL3 based on restriction enzyme cutting sites of BglII and Hin-dI-II. The pGL3-SP1 vector, pRL construction vector containing renilla luciferase reporter gene, pcDNA3.1 control, and pcDNA3.1-SP1 expression vector were co-transfected into 293T cells. Before transfection, 293T cells were seeded into a 6-well plate at a density of 5×10^5 cells/well. When reaching approximately 60% confluence, cells were transfected. After 48 h, Dual-Luciferase® Reporter Assay System (Promega Corporation, Madison, WI, USA) was used to detect the luciferase activity, which was expressed as the ratio of relative activity of firefly luciferase to that of renilla luciferase.

Statistical Analysis

All experimental data were processed using SPSS 21.0 statistical software (IBM Corp. Armonk, NY, USA). The measurement data were expressed as mean \pm standard deviation. Data between 2 groups were analyzed using unpaired *t* test, while data among multiple groups were assessed using one-way ANOVA, followed by Tukey's post hoc tests. Kaplan-Meier method was employed to evaluate the survival rate of mice, and log-rank test was used for single-factor analysis. $p < 0.05$ was considered to be statistical significance.

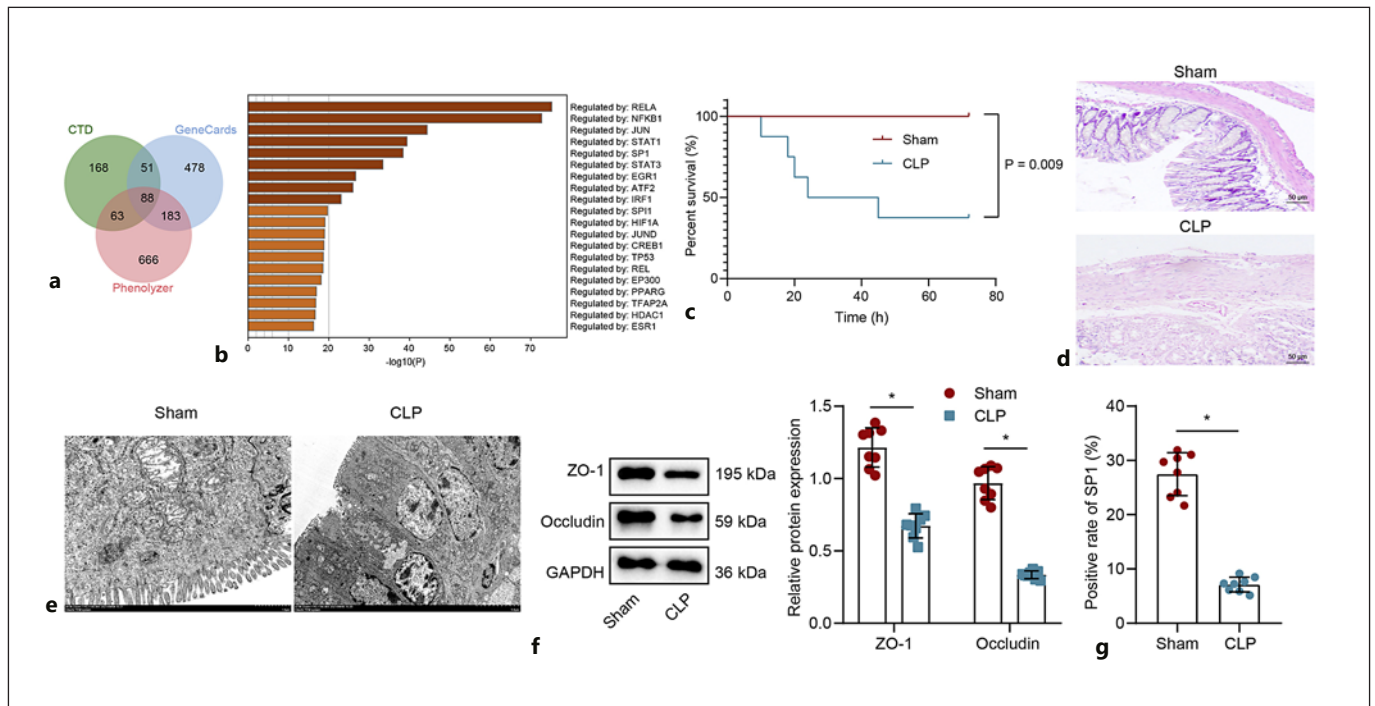


Fig. 1. Characterization of the CLP-induced mouse sepsis model and significance of SP1 in sepsis. **a** Venn diagram of the predicted genes related to sepsis by the CTD, GeneCards, and Phenolyzer databases. **b** A bar chart of regulatory factors of the obtained 88 candidate targets predicted by the Metascape database. **c** Survival rate of Sham-operated and septic mice. **d** HE staining analysis of intestinal tissues of Sham-operated and septic mice. **e** Pathological changes of intestinal tissues of Sham-operated and septic mice under a TEM. **f** Western blot analysis of ZO-1 and occludin proteins

in intestinal tissues of Sham-operated and septic mice. **g** Immunohistochemistry staining analysis of SP1 protein in intestinal tissues of Sham-operated and septic mice. $n = 8$ for Sham-operated and septic mice. $*p < 0.05$ between groups. The experiment was repeated 3 times independently. HE, hematoxylin-eosin; TEM, transmission electron microscope; CLP, cecal ligation perforation; SP1, specificity protein-1; GAPDH, glyceraldehyde-3-phosphate dehydrogenase.

Results

Identification of the CLP-Induced Mouse Sepsis Model and Downregulated SP1 in the Intestinal Tissues of CLP Mice

We first predicted the sepsis-related genes using the CTD (Inference Score >40 ; <http://ctdbase.org/detail.go?acc=C452899&type=chem>), GeneCards (screening the first 800 genes; <https://www.genecards.org/>), and Phenolyzer databases (screening the first 1,000 genes; <http://phenolyzer.wglab.org/>). The obtained results were analyzed with Venn diagram using the jvenn (<http://jvenn.toulouse.inra.fr/app/example.html>), which yielded 88 candidate targets (Fig. 1a). These targets were then subjected to enrichment analysis using the Metascape website (<https://metascape.org/gp/index.html#/main/step1>), which showed that the candidate targets could be regulated by SP1 (Fig. 1b).

In order to further explore the molecular mechanism by which SP1 regulates intestinal barrier in septic mice, we first constructed the mouse sepsis model by CLP. The septic mice exhibited decreased survival rate (Fig. 1c), shortened villi of intestinal mucosa, severe leukocyte infiltration, and reduced intestinal epithelial cells (Fig. 1d). Additionally, the intestinal mucosal epithelial cells were swollen, tight junctions were damaged, intercellular space was widened, and mitochondria were swollen in the intestinal tissues of septic mice (Fig. 1e). Western blot analysis revealed a decline in the expression of intestinal mucosal barrier marker proteins ZO-1 and occludin (Fig. 1f). These results demonstrated the successful establishment of the CLP mouse model. Analysis of immunohistochemistry suggested much lower SP1-positive expression in intestinal tissues of septic mice than Sham-operated mice (Fig. 1g), indicating the potential implication of SP1 in the regulation of intestinal barrier mucosal injury in sepsis.

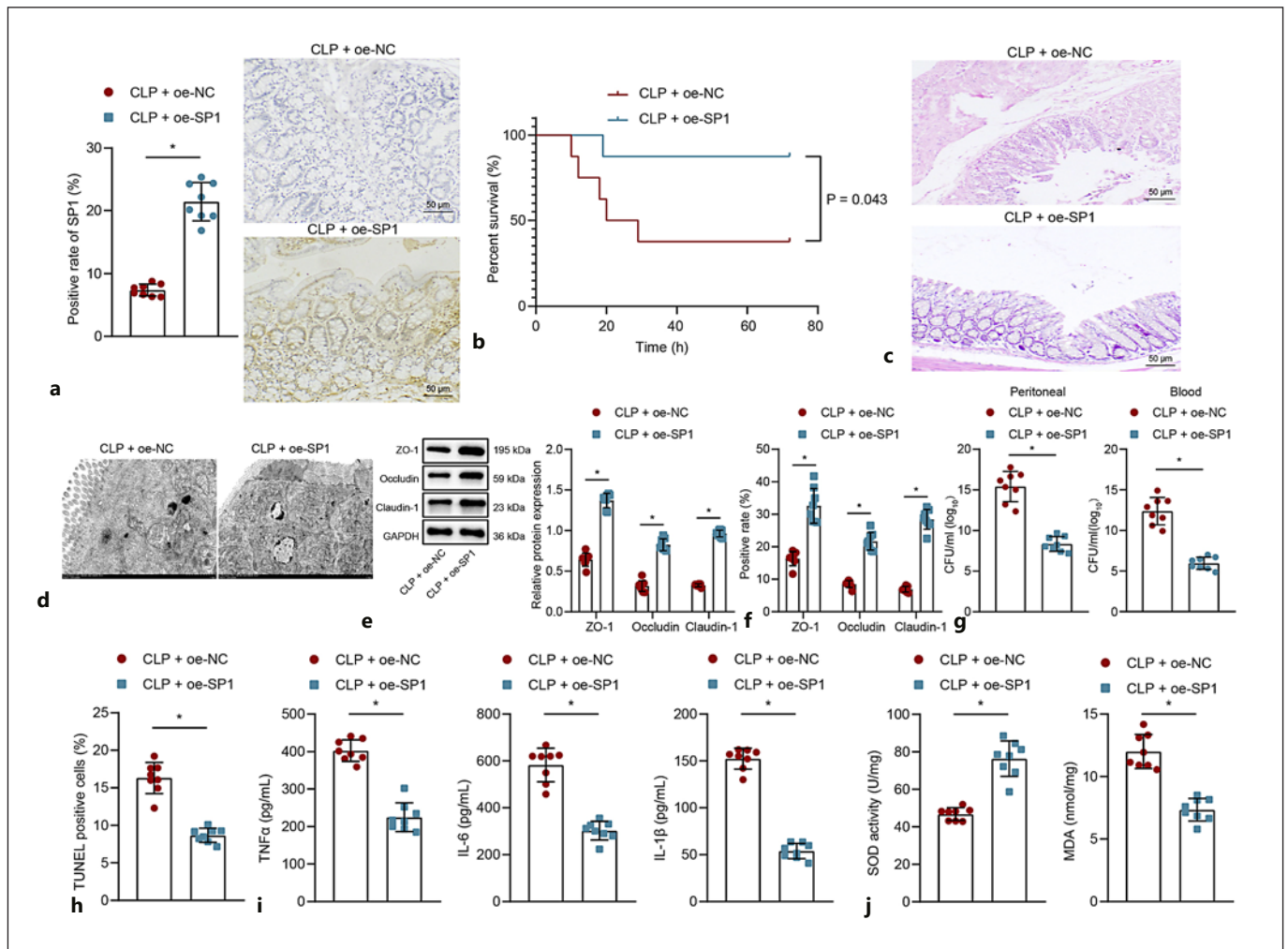


Fig. 2. Upregulation of SP1 improves intestinal barrier dysfunction and suppresses oxidative stress and epithelial cell apoptosis in septic mice. **a** Immunohistochemistry staining analysis of SP1 protein in intestinal tissues of septic mice treated with oe-SP1. **b** Survival rate of septic mice treated with oe-SP1. **c** HE staining analysis of intestinal tissues of septic mice treated with oe-SP1. **d** Pathological changes of intestinal tissues of septic mice treated with oe-SP1 under a TEM. **e** Western blot analysis of ZO-1, occludin, and claudin-1 proteins in intestinal tissues of septic mice treated with oe-SP1. **f** Immunohistochemistry staining analysis of ZO-1, occludin, and claudin-1 proteins in intestinal tissues of septic mice treated with oe-SP1. **g** Colony-forming unit in the PLF and serum of septic mice treated with oe-SP1. **h** Apoptosis of intestinal epithelial

cells measured by TUNEL assay. **i** Serum levels of TNF- α , IL-6, and IL-1 β in septic mice treated with oe-SP1 measured by ELISA. **j** MDA content and SOD activity in intestinal tissues of septic mice treated with oe-SP1. $n = 8$ for mice following each treatment. $*p < 0.05$ between groups. The experiment was repeated 3 times independently. HE, hematoxylin-eosin; TEM, transmission electron microscope; TUNEL, terminal deoxynucleotidyl transferase-mediated dUTP-biotin nick end labeling; SP1, specificity protein-1; PLF, peritoneal lavage fluid; ELISA, enzyme-linked immunosorbent assay; MDA, malondialdehyde; SOD, superoxide dismutase; CLP, cecal ligation perforation; oe-NC, overexpression-negative control; GAPDH, glyceraldehyde-3-phosphate dehydrogenase.

Overexpression of SP1 Attenuates Intestinal Barrier Dysfunction, Oxidative Stress, and Epithelial Cell Apoptosis in CLP Mice

Next, we further dissected out the role of SP1 in the intestinal barrier dysfunction in septic mice. Immunohistochemistry showed that the positive expression of SP1

was increased in intestinal tissues of septic mice overexpressing SP1 (Fig. 2a). Additionally, upon SP1 overexpression, the survival rate of septic mice was increased (Fig. 2b), the intestinal mucosa was intact, the villi were arranged orderly, and leukocyte infiltration was reduced (Fig. 2c). Meanwhile, the morphology intestinal epithe-

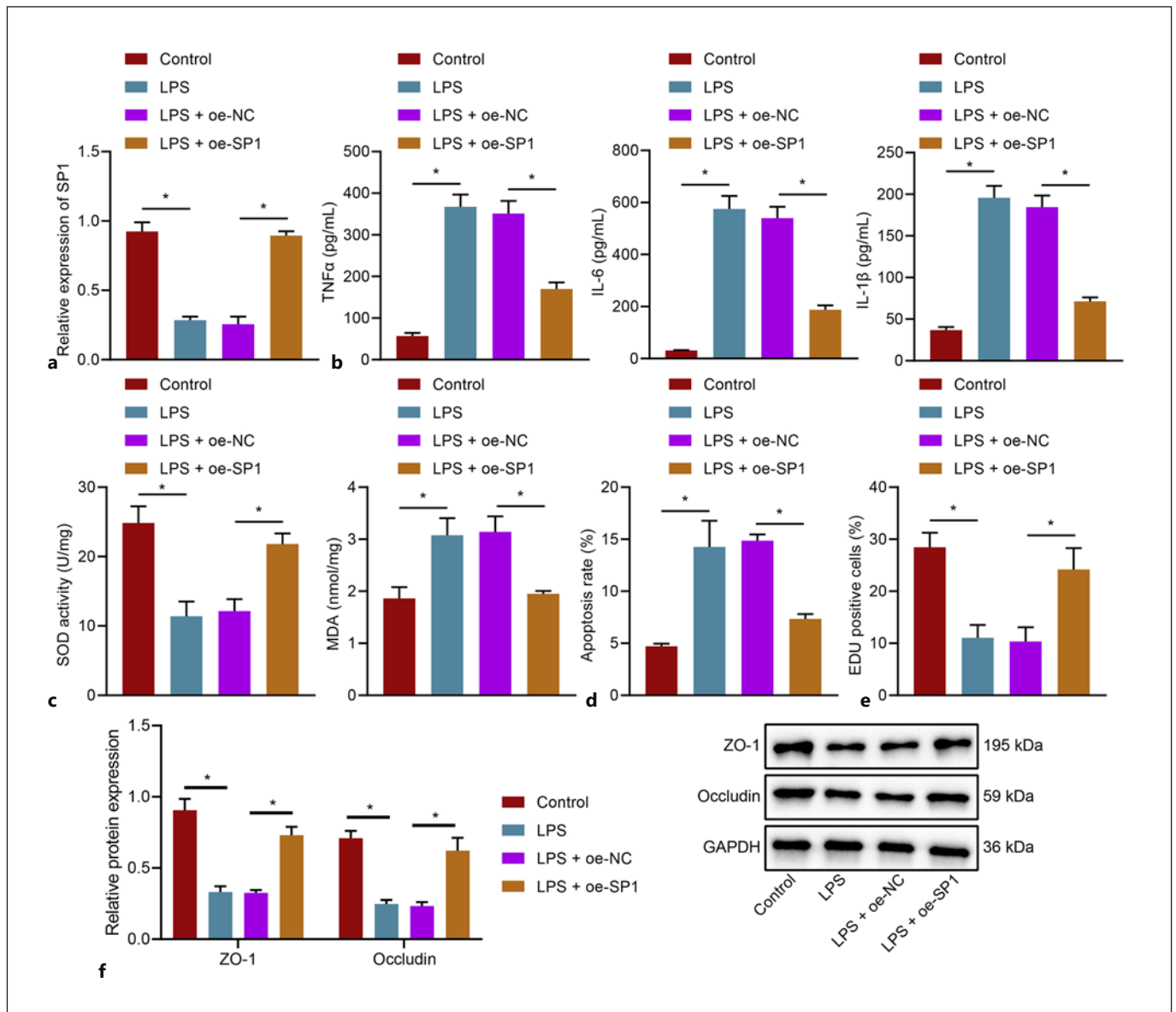


Fig. 3. Upregulation of SP1 suppresses LPS-induced inflammatory response, oxidative stress, and apoptosis of intestinal epithelial cells. **a** SP1 mRNA expression determined by RT-qPCR in LPS-induced cells transfected with oe-SP1. **b** Levels of TNF- α , IL-6, and IL-1 β measured by ELISA in the culture medium of LPS-induced cells transfected with oe-SP1. **c** MDA content and SOD activity in LPS-induced cells transfected with oe-SP1. **d** Flow cytometric analysis of the apoptosis rate of LPS-induced cells transfected with oe-SP1. **e** Proliferation of LPS-induced cells transfected with oe-

SP1 measured by EdU assay. **f** Western blot analysis of ZO-1 and occludin proteins in LPS-induced cells transfected with oe-SP1. * $p < 0.05$ between groups. The experiment was repeated 3 times independently. RT-qPCR, reverse transcription-quantitative polymerase chain reaction; SP1, specificity protein-1; LPS, lipopolysaccharide; ELISA, enzyme-linked immunosorbent assay; MDA, malondialdehyde; SOD, superoxide dismutase; GAPDH, glyceraldehyde-3-phosphate dehydrogenase; oe-NC, overexpression-negative control.

lial cells were normal and the tight junctions were arranged orderly following SP1 overexpression (Fig. 2d).

Western blot analysis showed an enhancement of the expression of ZO-1, occludin, and claudin-1 proteins in

intestinal tissues of septic mice treated with oe-SP1 (Fig. 2e). Similar results were also observed at the positive expression revealed by immunohistochemistry (Fig. 2f). The colony-forming unit was found to be reduced in the

presence of SP1 overexpression (Fig. 2g). Moreover, TUNEL staining showed a downward trend in the apoptosis rate of intestinal epithelial cells (Fig. 2h), serum levels of TNF- α , IL-6, and IL-1 β (Fig. 2i), and MDA content (Fig. 2j), while SOD activity (Fig. 2j) was elevated in septic mice treated with oe-SP1. These findings suggested that overexpression of SP1 prevented intestinal barrier dysfunction, oxidative stress, and epithelial cell apoptosis in septic mice.

SP1 Reduces LPS-Induced Inflammatory Factor Release, Oxidative Stress, and Apoptosis in Intestinal Epithelial Cells

We overexpressed SP1 in LPS-induced MODE-K cells to validate the effect of SP1 in vitro. The results of RT-qPCR showed that the expression of SP1 was inhibited in MODE-K cells following LPS treatment, while it was augmented following oe-SP1 transfection (Fig. 3a). ELISA results revealed that the levels of TNF- α , IL-6, and IL-1 β were elevated in the cell culture medium upon LPS treatment, which was reversed in response to overexpression of SP1 (Fig. 3b). In addition, LPS treatment led to increased MDA content and decreased SOD activity, while overexpression of SP1 abolished the effect of LPS (Fig. 3c).

The apoptosis rate of LPS-induced cells was increased, and the increase was then abrogated by SP1 overexpression (Fig. 3d). The results of EdU staining demonstrated a decline of cell proliferation upon LPS treatment, whereas overexpression of SP1 promoted cell proliferation (Fig. 3e). Further, LPS was observed to decrease the protein expression ZO-1 and occludin, while overexpression of SP1 negated the trend (Fig. 3f). Cumulatively, SP1 could attenuate LPS-induced inflammatory response, oxidative stress, and apoptosis of intestinal epithelial cells.

SP1 Enhances the Transcription of HDAC4, Promotes Deacetylation of HMGB1, and Induces Its Translocation into Nuclei

We then elucidated the downstream mechanism of SP1 in sepsis. The GeneCards database was initially used to retrieve SP1-related genes, and the first 25 genes were analyzed by constructing a protein-protein interaction network using the String database (<http://string-db.org/cgi/input.pl>) and Cytoscape 3.5.1 (Fig. 4a). By screening degree > Avg (Degree), 15 candidate genes were identified. Additionally, we retrieved 472 downstream target genes of SP1 from the TRRUST database (<https://www.grnpedia.org/trrust/>), which were subjected to Venn diagram analysis with the aforesaid 15 candidate genes, and

3 target genes (EGR1, HDAC4, and RELA) were thereby identified at the intersection (Fig. 4b).

Previous literature revealed that SP1 could bind to the promoter region of HDAC4 to promote its transcriptional activation, and meanwhile, HDAC4 inhibited the occurrence of sepsis [9, 11]. Therefore, we chose HDAC4 as the SP1 downstream target for the following experiment. Prediction results of the ChIPBase database (<http://rna.sysu.edu.cn/chipbase/index.php>) revealed the binding sites of SP1 in the HDAC4 (Fig. 4c). Chromatin immunoprecipitation (ChIP) analysis showed that SP1 was enriched in the HDAC4 promoter (Fig. 4d), and dual-luciferase reporter assay further demonstrated that the luciferase activity of HDAC4 promoter was increased in 293T cells upon SP1 overexpression (Fig. 4e). Furthermore, HDAC4 mRNA and protein expressions were determined to be enhanced in SP1-overexpressing MODE-K cells (Fig. 4f, g).

Prediction results of the GeneCards and BioGRID (<https://thebiogrid.org/>) databases revealed 2,369 and 391 HDAC4-related genes, respectively. These genes were then intersected with the sepsis-related genes, with 11 genes (CDKN1A, NFKBIA, HMGB1, MAPK3, STAT1, MAPK1, PPARG, HIF1A, CTNNA1, APP, and SP1) obtained (Fig. 4h). Next, the Multi-Experiment Matrix tool (<https://biit.cs.ut.ee/mem/index.cgi>) was employed to analyze the correlation among HDAC4 and these candidate-related genes, which were sorted and aggregated using robust rank aggregation method [17]. As illustrated in Figure 4i, MAPK1 and HMGB1 showed the most significant correlation with HDAC4 according to the *p* value. Interestingly, it has been previously reported that the inhibition of HDAC4 could promote the acetylation of HMGB1, while inhibition of HMGB1 can protect intestinal barrier [18, 19]. Therefore, we speculated that the interaction between HDAC4 and HMGB1 may participate in the regulation of SP1 on intestinal barrier function during sepsis. Subsequent results of immunohistochemistry displayed decreased HDAC4-positive expression rate and increased HMGB1-positive expression rate in intestinal tissues of septic mice (Fig. 4j). Immunoprecipitation results showed that LPS treatment promoted HMGB1 protein expression and acetylation level, while further overexpression of HDAC4 abolished this trend in cells (Fig. 4k). In addition, the experimental results from fractionation of nuclear/cytoplasmic RNA suggested that SP1 overexpression triggered the HMGB1 translocation into nuclei (Fig. 4l). It was also observed that HDAC4 overexpression facilitated the HMGB1 translocation into nuclei (Fig. 4m), and consistently, immunofluorescence

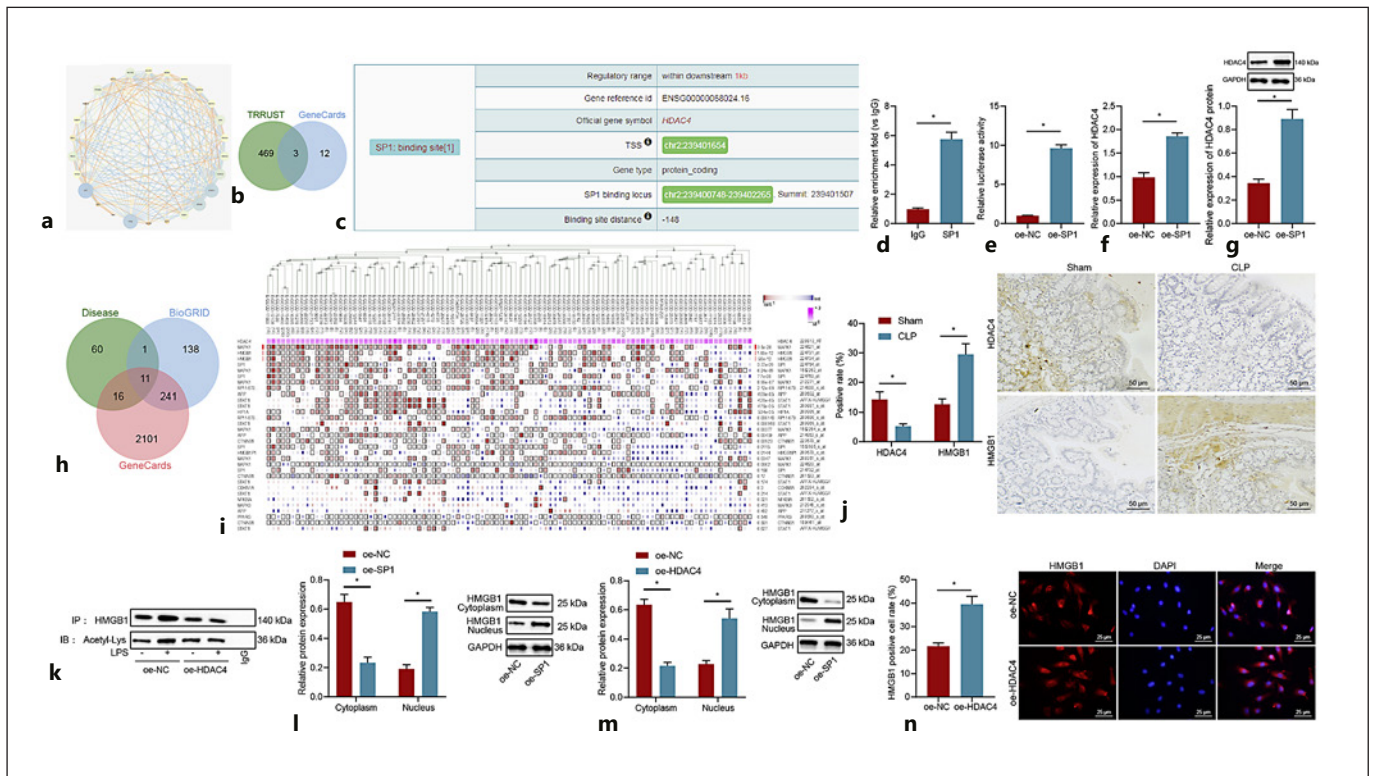


Fig. 4. SP1 increases HDAC4 transcription and expression, causing inhibition of HMGB1 acetylation level and its translocation into nuclei. **a** PPI network of the SP1-related genes predicted by the GeneCards database. **b** Venn diagram of the downstream target genes of SP1 analyzed by the TRRUST database and SP1-related genes. **c** Binding sites of SP1 in the HDAC4 predicted by the ChIPBase database. **d** SP1 enrichment in the HDAC4 promoter analyzed by ChIP. **e** Binding of SP1 to HDAC4 confirmed by dual-luciferase reporter assay in 293T cells. **f** HDAC4 mRNA expression determined by RT-qPCR in MODE-K cells transfected with oe-SP1. **g** Western blot analysis of HDAC4 protein in MODE-K cells transfected with oe-SP1. **h** Venn diagram of the HDAC4-related genes analyzed by the GeneCards and BioGRID databases and sepsis-related genes. **i** The interaction between HDAC4 and other genes analyzed by MEM dataset; each square represents a sample. **j** Immunohistochemistry staining analysis of HDAC4 and HMGB1 proteins in intestinal tissues of septic mice. **k** Immuno-

precipitation analysis of HMGB1 protein and acetylation level in oe-HDAC4-transfected MODE-K cells. **l** HMGB1 translocation into nuclei analyzed by fractionation of nuclear/cytoplasmic RNA in SP1-overexpressing MODE-K cells. **m** HMGB1 translocation into nuclei analyzed by fractionation of nuclear/cytoplasmic RNA in HDAC4-overexpressing MODE-K cells. **n** Immunofluorescence analysis of HMGB1 protein in HDAC4-overexpressing MODE-K cells. * $p < 0.05$ between groups. The experiment was repeated 3 times independently. RT-qPCR, reverse transcription-quantitative polymerase chain reaction; ChIP, chromatin immunoprecipitation; PPI, protein-protein interaction; MEM, Multi-Experiment Matrix; SP1, specificity protein-1; HDAC4, histone deacetylase 4; HMGB1, high mobility group box 1; oe-NC, overexpression-negative control; GAPDH, glyceraldehyde-3-phosphate dehydrogenase; CLP, cecal ligation perforation; LPS, lipopolysaccharide.

results demonstrated the similar result (Fig. 4n). These results indicated that SP1 augmented HDAC4 transcription and expression, inducing inhibited HMGB1 acetylation level and its translocation into nuclei.

SP1 Reduces Inflammatory Response, Oxidative Stress, and Apoptosis of Intestinal Epithelial Cells via HDAC4-Mediated Deacetylation of HMGB1

We then proceeded to examine the effect of the SP1/HDAC4/HMGB1 axis on intestinal mucosal injury. The

results of RT-qPCR showed upregulated mRNA expression of HDAC4 and SP1 in LPS-induced MODE-K cells overexpressing SP1, while simultaneous overexpression of SP1 and HMGB1 led to increased HMGB1 mRNA expression. HDAC4 expression was decreased in response to the combined transfection of oe-SP1 and si-HDAC4 plasmids as compared with oe-SP1 alone (Fig. 5a). Western blot analysis and immunoprecipitation analysis illustrated that the protein expression of SP1 and HDAC4 was augmented but HMGB1 protein expression and acetylation level were

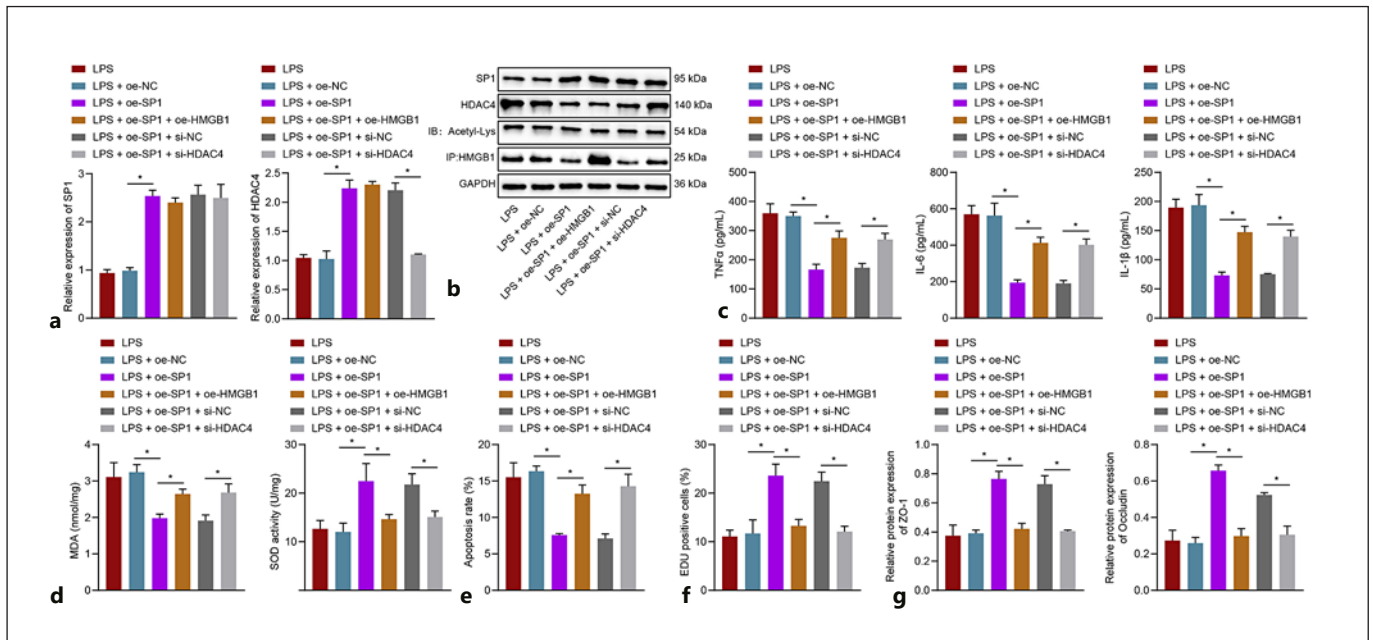


Fig. 5. SP1 advances HDAC4-mediated HMGB1 deacetylation and prevents inflammatory response, oxidative stress, and apoptosis of intestinal epithelial cells. LPS-induced MODE-K cells were transfected with oe-SP1, oe-SP1 + oe-HMGB1, or oe-SP1 + si-HDAC4. **a** SP1 and HDAC4 mRNA expressions determined by RT-qPCR in MODE-K cells. **b** HDAC4 protein expression and acetylation level determined by Western blot analysis and immunoprecipitation assay in MODE-K cells. **c** TNF- α , IL-6, and IL-1 β expressions determined by ELISA in the supernatant of MODE-K cells. **d** MDA content and SOD activity in MODE-K cells. **e** Flow cyto-

metric analysis of the apoptosis rate of MODE-K cells. **f** Proliferation of MODE-K cells measured by EdU assay. **g** Western blot analysis of ZO-1 and occludin proteins in MODE-K cells. * $p < 0.05$ between groups. The experiment was repeated 3 times independently. RT-qPCR, reverse transcription-quantitative polymerase chain reaction; SP1, specificity protein-1; HDAC4, histone deacetylase 4; HMGB1, high mobility group box 1; LPS, lipopolysaccharide; oe-NC, overexpression-negative control; GAPDH, glyceraldehyde-3-phosphate dehydrogenase; MDA, malondialdehyde.

decreased in the presence of SP1 overexpression. No changes were found in the HMGB1 acetylation level, but its protein expression was upregulated upon simultaneous overexpression of SP1 and HMGB1. Additionally, HDAC4 was decreased, while the HMGB1 protein expression and acetylation level were increased following combined treatment with oe-SP1 and si-HDAC4 (Fig. 5b).

ELISA data showed that TNF- α , IL-6, and IL-1 β expressions were decreased in the supernatant of LPS-induced cells overexpressing SP1, while it was upregulated following combined treatment with oe-SP1 and oe-HMGB1 or oe-SP1 and si-HDAC4 (Fig. 5c). Moreover, overexpression of SP1 reduced the MDA content while increasing the SOD activity, the effect of which was counteracted upon additional HMGB1 overexpression or HDAC4 silencing (Fig. 5d). Similarly, the diminished cell apoptosis and augmented cell proliferation induced by SP1 overexpression could be reverted by further treatment with oe-HMGB1 or si-HDAC4 (Fig. 5e, f). Meanwhile, the promoting effect of SP1 overexpression on the

protein expression of ZO-1 and occludin was abrogated following dual treatment with oe-SP1 and oe-HMGB1 or oe-SP1 and si-HDAC4 (Fig. 5g). The aforementioned data supported that SP1 could attenuate inflammatory response, oxidative stress, and apoptosis of intestinal epithelial cells via promotion of HDAC4-mediated deacetylation of HMGB1.

HMGB1 Knockdown Hinders Intestinal Barrier Injury, Oxidative Stress, and Inflammatory Response in CLP Mice

Finally, we further performed in vivo assays to validate the aforementioned effect of SP1 through HDAC4-mediated deacetylation of HMGB1. The results of immunohistochemistry showed a decline of HMGB1-positive expression rate in intestinal tissues of septic mice with HMGB1 knockdown (Fig. 6a). Additionally, the survival rate of septic mice was observed to be increased upon HMGB1 knockdown (Fig. 6b). Analysis on the intestinal tissues using hematoxylin-eosin (HE) staining and transmission

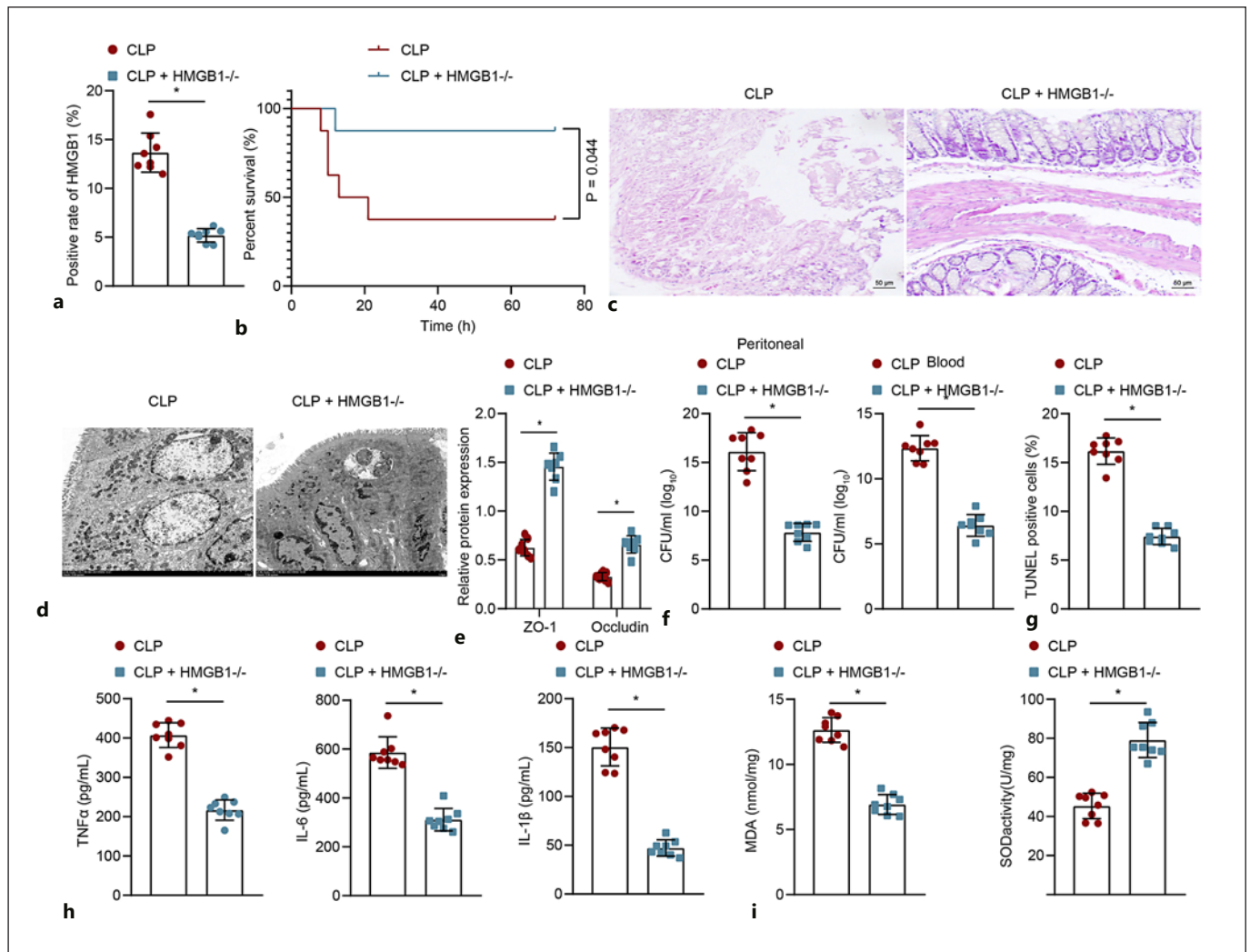


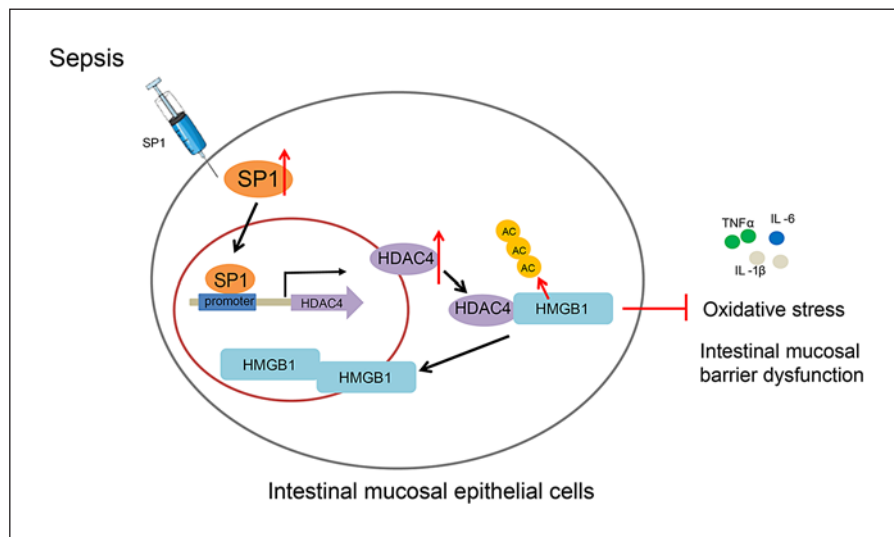
Fig. 6. HMGB1 knockdown delays the intestinal barrier injury, oxidative stress, and inflammatory response in septic mice. **a** Immunohistochemistry staining analysis of HMGB1 protein in intestinal tissues of HMGB1^{-/-} septic mice. **b** Survival rate of HMGB1^{-/-} septic mice. **c** HE staining analysis of intestinal tissues of HMGB1^{-/-} septic mice. **d** Pathological changes of intestinal tissues of HMGB1^{-/-} septic mice under a TEM. **e** Western blot analysis of ZO-1 and occludin proteins in intestinal tissues of HMGB1^{-/-} septic mice. **f** Colony-forming unit in the PLF and serum of HMGB1^{-/-} septic mice. **g** Apoptosis of intestinal epithelial cells in intestinal tissues of HMGB1^{-/-} septic mice measured by TUNEL assay.

h Serum levels of TNF- α , IL-6, and IL-1 β in HMGB1^{-/-} septic mice measured by ELISA. **i** MDA content and SOD activity in intestinal tissues of HMGB1^{-/-} septic mice. $n = 8$ for mice following each treatment. $*p < 0.05$ between groups. The experiment was repeated 3 times independently. HE, hematoxylin-eosin; TEM, transmission electron microscope; TUNEL, Terminal deoxynucleotidyl transferase-mediated dUTP-biotin nick end labeling; HMGB1, high mobility group box 1; PLF, peritoneal lavage fluid; ELISA, enzyme-linked immunosorbent assay; MDA, malondialdehyde; SOD, superoxide dismutase; CLP, cecal ligation perforation.

electron microscope (TEM) suggested relatively intact intestinal mucosa, arranged orderly villi, decreased leukocyte infiltration (Fig. 6c), normal epithelial cells, and well-arranged tight junctions following HMGB1 knockdown (Fig. 6d). Further, the protein expression of ZO-1 and occludin was elevated in intestinal tissues of HMGB1^{-/-} septic mice (Fig. 6e). There was a decreased number of colo-

ny-forming units in PLF and serum of HMGB1^{-/-} septic mice (Fig. 6f). Meanwhile, HMGB1 knockdown resulted in a decline of cell apoptosis (Fig. 6g), serum levels of TNF- α , IL-6, and IL-1 β (Fig. 6h), and MDA content while augmenting the SOD activity (Fig. 6i). Therefore, HMGB1 knockdown could impair the intestinal barrier injury, oxidative stress, and inflammatory response in septic mice.

Fig. 7. The mechanism diagram of SP1/HDAC4/HMGB1 axis in sepsis. SP1 stimulated the HDAC4 transcription and decreased HMGB1 level and its translocation into nuclei, consequently preventing intestinal barrier dysfunction, oxidative stress, and inflammatory response, therefore delaying the progression of sepsis. HMGB1, high mobility group box 1; SP1, specificity protein-1; HDAC4, histone deacetylase 4.



Discussion

Sepsis represents the main cause of death in critically ill patients [20]. SP1 has been involved in human diseases due to its regulation in the expression of genes associated with a wide range of cellular processes in mammalian cells [6]. The aim of the present study was to investigate the role of SP1 in the progression of sepsis. Through pre-experiment and confirmation, this study suggested that SP1 stimulated the HDAC4 transcription and decreased HMGB1 acetylation level and its translocation into nuclei, consequently preventing intestinal barrier dysfunction, oxidative stress, and inflammatory response, therefore delaying the progression of sepsis.

Initial results in the present study revealed downregulated SP1 expression in the intestinal tissues of septic mice. In line with this, the protein level of SP1 has been detected to be decreased by LPS treatment in human umbilical vein endothelial cells during sepsis [21]. Inflammatory response and oxidative stress have been shown to play an important role in the pathophysiological process of sepsis [22]. Enhanced SP1 activity has anti-inflammatory effects since it can increase the level of IL-10 and decrease that of TNF- α in the lung tissues exposed to LPS [23]. The present results suggested that SP1 reduced MDA content while augmenting the SOD activity. MDA and SOD are 2 typical markers often used to examine the level of oxidative stress [24], of which MDA content is upregulated while SOD activity is downregulated in the liver tissue of septic mice [25]. As known, sepsis could lead to the mutations of the symbiotic intestinal microenvironment, causing a dysbi-

otic environment, which further promote the hyperinflammation, hyperpermeability, and apoptosis of epithelial cells, and domination of pathogenic bacteria [26]. SP1, a ubiquitous nuclear factor in eukaryotic cells, may play essential roles in the regulation of di-/tripeptide absorption in the intestine [27]. Furthermore, it has been indicated that SP1 can increase the claudin-1 transcription to enhance intestinal barrier function, which is essential for the maintenance of normal intestinal function [28]. SP1 acetylation driven by HDAC inhibitors loses p21 and bak promoter binding function and results in death of intestinal epithelial cells [29]. These findings proved the inhibiting effect of SP1 overexpression on the intestinal barrier dysfunction, oxidative stress, and intestinal epithelial cell apoptosis following sepsis.

Mechanistic investigations in the current study indicated that SP1 enhanced the transcription of HDAC4 to promote deacetylation of HMGB1 and induce its translocation into nuclei. A previous study validated the binding sites for SP1 transcription factor in the HDAC4 promoter, and restored expression of SP1 contributes to upregulated HDAC4 protein expression in human cells [30]. In addition, increased HMGB1 acetylation levels are concomitant with a decrease of HDAC activity, indicating that HDAC activity inhibition triggers the increase of acetylated HMGB1 release following oxidative stress in hepatocytes [18]. It has been reported that *Entamoeba histolytica* HMGB1, a bona fide HMGB protein, shows the ability to regulate the parasite adaptation to the host intestine and affect the destruction of the host intestine [31]. The increase of HMGB1 in the jejunum tissues of

sepsis rats was identified [32]. Also, the suppression of HMGB1 underlies the improved intestinal mucosal barrier dysfunction in severe acute pancreatitis [19]. Acetylation of HMGB1 can prevent its entry into the nuclei and induce its secretion from the cell in which it can cause inflammation [33]. In agreement with our findings, up-regulated HDAC4 inhibits the acetylation and secretion of HMGB1 in both RAW264.7 cells and murine peritoneal macrophages following sepsis [13]. Meanwhile, LPS stimulation leads to a dramatic increase of HMGB1 expression, intracellular translocation, and acetylation level in a rat model of sepsis-associated liver damage [34]. Furthermore, decreased HMGB1 by miR-103a-3p blunts the inflammatory response and lung and liver tissue apoptosis while enhancing the survival rate of LPS-induced mouse sepsis models [35]. Importantly, SP1 binds to the promoter of HMGB1 and further recruits NcoR1 to negatively regulate the expression of HMGB1 in cell models of sepsis-induced myocardial dysfunction [36]. Cumulatively, it could be inferred that SP1 reduced inflammatory response, oxidative stress, and intestinal barrier dysfunction via HDAC4-mediated deacetylation of HMGB1.

Collectively, the present study revealed the mechanism underlying the involvement of SP1 in inflammatory response, oxidative stress, and intestinal barrier dysfunction following sepsis (Fig. 7), thus laying the basis for the development of novel therapeutic targets for the treatment of sepsis. However, further studies are still required to investigate the value of SP1 in sepsis based on human intestinal tissues to further validate it as a novel therapeutic target for the sepsis.

Acknowledgments

We would like to show sincere appreciation to our colleagues for helpful comments on this article.

References

- 1 Taeb AM, Hooper MH, Marik PE. Sepsis: current definition, pathophysiology, diagnosis, and management. *Nutr Clin Pract*. 2017; 32(3):296–308.
- 2 Yoseph BP, Klingensmith NJ, Liang Z, Breed ER, Burd EM, Mittal R, et al. Mechanisms of intestinal barrier dysfunction in sepsis. *Shock*. 2016;46(1):52–9.
- 3 Xie S, Yang T, Wang Z, Li M, Ding L, Hu X, et al. Astragaloside IV attenuates sepsis-induced intestinal barrier dysfunction via suppressing RhoA/NLRP3 inflammasome signaling. *Int Immunopharmacol*. 2020;78:106066.
- 4 Berretta M, Quagliariello V, Maurea N, Di Francia R, Sharifi S, Facchini G, et al. Multiple effects of ascorbic acid against chronic diseases: updated evidence from preclinical and clinical studies. *Antioxidants*. 2020;9(12):1182.
- 5 Kumar S, Tripathy S, Jyoti A, Singh SG. Recent advances in biosensors for diagnosis and detection of sepsis: a comprehensive review. *Biosens Bioelectron*. 2019;124–125:205–15.
- 6 Jain S. Sepsis: an update on current practices in diagnosis and management. *Am J Med Sci*. 2018;356(3):277–86.
- 7 O'Connor L, Gilmour J, Bonifer C. The role of the ubiquitously expressed transcription factor Sp1 in tissue-specific transcriptional regulation and in disease. *Yale J Biol Med*. 2016; 89(4):513–25.
- 8 Beishline K, Azizkhan-Clifford J. Sp1 and the “hallmarks of cancer.” *FEBS J*. 2015;282(2): 224–58.
- 9 An Y, Ni Y, Xu Z, Shi S, He J, Liu Y, et al. TRIM59 expression is regulated by Sp1 and Nrf1 in LPS-activated macrophages through JNK signaling pathway. *Cell Signal*. 2020;67: 109522.

Statement of Ethics

The current study was approved by the Ethics Committee of Shenzhen People's Hospital, the Second Clinical Medical College of Jinan University, the First Affiliated Hospital of South University of Science and Technology, and conducted according to the Guide for the Care and Use of Laboratory Animals published by the US National Institutes of Health. All efforts were made to minimize the number and suffering of the included animals.

Conflict of Interest Statement

The authors have no conflicts of interest relevant to this article.

Funding Sources

This study was supported by Guangdong Natural Science Foundation Project (No. 2021A1515012119), Shenzhen Key Laboratory Construction Fund, Shenzhen Key Medical Discipline Construction Fund, Youth Science Fund of National Science Foundation of China (81901771), and Science and Technology Project of Shenzhen (JCYJ20190807144209381).

Author Contributions

Zhen-Mi Liu, Xi Wang, Chen-Xi Li, and Xue-Yan Liu designed the study. Xiao-Jing Guo collated the data. Yang Li designed and developed the database. You-Lian Chen carried out data analyses and produced the initial draft of the manuscript. Zhen-Mi Liu, Hong-Xing Ye, and Huai-Sheng Chen contributed to drafting the manuscript. All authors have read and approved the final submitted manuscript.

Data Availability Statement

The datasets generated/analyzed during the current study are available.

- 10 Guida N, Laudati G, Mascolo L, Valsecchi V, Sirabella R, Selleri C, et al. p38/Sp1/Sp4/HDAC4/BDNF axis is a novel molecular pathway of the neurotoxic effect of the methylmercury. *Front Neurosci*. 2017;11:8.
- 11 Wang Z, Qin G, Zhao TC. HDAC4: mechanism of regulation and biological functions. *Epigenomics*. 2014;6(1):139–50.
- 12 Formisano L, Laudati G, Guida N, Mascolo L, Serani A, Cuomo O, et al. HDAC4 and HDAC5 form a complex with DREAM that epigenetically down-regulates NCX3 gene and its pharmacological inhibition reduces neuronal stroke damage. *J Cereb Blood Flow Metab*. 2020;40(10):2081–97.
- 13 Park EJ, Kim YM, Kim HJ, Chang KC. Degradation of histone deacetylase 4 via the TLR4/JAK/STAT1 signaling pathway promotes the acetylation of high mobility group box 1 (HMGB1) in lipopolysaccharide-activated macrophages. *FEBS Open Bio*. 2018;8(7):1119–26.
- 14 Gentile LF, Moldawer LL. HMGB1 as a therapeutic target for sepsis: it's all in the timing!. *Expert Opin Ther Targets*. 2014;18(3):243–5.
- 15 Vidyanti AN, Hsieh JY, Lin KJ, Fang YC, Setyopranoto I, Hu CJ. Role of HMGB1 in an animal model of vascular cognitive impairment induced by chronic cerebral hypoperfusion. *Int J Mol Sci*. 2020;21(6):2176.
- 16 Xue J, Patergnani S, Giorgi C, Suarez J, Goto K, Bononi A, et al. Asbestos induces mesothelial cell transformation via HMGB1-driven autophagy. *Proc Natl Acad Sci U S A*. 2020;117(41):25543–52.
- 17 Kolde R, Laur S, Adler P, Vilo J. Robust rank aggregation for gene list integration and meta-analysis. *Bioinformatics*. 2012;28(4):573–80.
- 18 Evankovich J, Cho SW, Zhang R, Cardinal J, Dhupar R, Zhang L, et al. High mobility group box 1 release from hepatocytes during ischemia and reperfusion injury is mediated by decreased histone deacetylase activity. *J Biol Chem*. 2010;285(51):39888–97.
- 19 Chen X, Zhao HX, Bai C, Zhou XY. Blockade of high-mobility group box 1 attenuates intestinal mucosal barrier dysfunction in experimental acute pancreatitis. *Sci Rep*. 2017;7(1):6799.
- 20 Yang Y, Xie JF, Yu KJ, Yao C, Li JG, Guan XD, et al. Epidemiological study of sepsis in china: protocol of a cross-sectional survey. *Chin Med J*. 2016;129(24):2967–73.
- 21 Liu W, Zhu ZQ, Wang W, Zu SY, Zhu GJ. Crucial roles of GATA-2 and SP1 in adrenomedullin-affected expression of tissue factor pathway inhibitor in human umbilical vein endothelial cells exposed to lipopolysaccharide. *Thromb Haemost*. 2007;97(5):839–46.
- 22 Kashiouris MG, L'Heureux M, Cable CA, Fisher BJ, Leichtle SW, Fowler AA. The emerging role of vitamin C as a treatment for sepsis. *Nutrients*. 2020;12(2):292.
- 23 Ye X, Liu H, Gong YS, Liu SF. LPS down-regulates specificity protein 1 activity by activating NF-kappaB pathway in endotoxemic mice. *PLoS One*. 2015;10(6):e0130317.
- 24 Gong W, Zhu G, Li J, Yang X. LncRNA MALAT1 promotes the apoptosis and oxidative stress of human lens epithelial cells via p38MAPK pathway in diabetic cataract. *Diabetes Res Clin Pract*. 2018;144:314–21.
- 25 Jin W, Zhao Y, Hu Y, Yu D, Li X, Qin Y, et al. Stromal cell-derived factor-1 enhances the therapeutic effects of human endometrial regenerative cells in a mouse sepsis model. *Stem Cells Int*. 2020;2020:4820543.
- 26 Fay KT, Ford ML, Coopersmith CM. The intestinal microenvironment in sepsis. *Biochim Biophys Acta Mol Basis Dis*. 2017;1863(10 Pt B):2574–83.
- 27 Qu F, Tang J, Hu R, Hao G, Zhou Y, Lu S, et al. Molecular characterization and nutritional regulation of specificity protein 1 (Sp1) in grass carp (*Ctenopharyngodon idella*). *Aquac Nutr*. 2018;24(3):940–51.
- 28 Wang HB, Wang PY, Wang X, Wan YL, Liu YC. Butyrate enhances intestinal epithelial barrier function via up-regulation of tight junction protein Claudin-1 transcription. *Dig Dis Sci*. 2012;57(12):3126–35.
- 29 Waby JS, Chirakkal H, Yu C, Griffiths GJ, Benson RS, Bingle CD, et al. Sp1 acetylation is associated with loss of DNA binding at promoters associated with cell cycle arrest and cell death in a colon cell line. *Mol Cancer*. 2010;9:275.
- 30 Liu F, Pore N, Kim M, Voong KR, Dowling M, Maity A, et al. Regulation of histone deacetylase 4 expression by the SP family of transcription factors. *Mol Biol Cell*. 2006;17(2):585–97.
- 31 Abhyankar MM, Hochreiter AE, Hershey J, Evans C, Zhang Y, Crasta O, et al. Characterization of an Entamoeba histolytica high-mobility-group box protein induced during intestinal infection. *Eukaryot Cell*. 2008;7(9):1565–72.
- 32 Wu JN, Wu W, Jiang RL, Zhu MF, Lei S, Lu B. [Effect of electro-acupuncture at zusanli (ST36) on the expression of ghrelin and HMGB1 in the small intestine of sepsis rats]. *Zhongguo Zhong Xi Yi Jie He Za Zhi*. 2014;34(9):1113–7. Chinese.
- 33 Yang H, Antoine DJ, Andersson U, Tracey KJ. The many faces of HMGB1: molecular structure-functional activity in inflammation, apoptosis, and chemotaxis. *J Leukoc Biol*. 2013;93(6):865–73.
- 34 Tian T, Yao D, Zheng L, Zhou Z, Duan Y, Liu B, et al. Sphingosine kinase 1 regulates HMGB1 translocation by directly interacting with calcium/calmodulin protein kinase II- δ in sepsis-associated liver injury. *Cell Death Dis*. 2020;11(12):1037.
- 35 Li Y, Zhu H, Pan L, Zhang B, Che H. microRNA-103a-3p confers protection against lipopolysaccharide-induced sepsis and consequent multiple organ dysfunction syndrome by targeting HMGB1. *Infect Genet Evol*. 2021;89:104681.
- 36 Peng Q, Xu H, Xiao M, Wang L. The small molecule PSSM0332 disassociates the CRL4A(DCAF8) E3 ligase complex to decrease the ubiquitination of NcoR1 and inhibit the inflammatory response in a mouse sepsis-induced myocardial dysfunction model. *Int J Biol Sci*. 2020;16(15):2974–88.